Journal of Cerebral Blood Flow & Metabolism (2015) 35, 655–666

www.jcbfm.com

ORIGINAL ARTICLE

The nuclear splicing factor RNA binding motif 5 promotes caspase activation in human neuronal cells, and increases after traumatic brain injury in mice

Travis C Jackson[1], Lina Du[1], Keri Janesko-Feldman[1], Vincent A Vagni[1], Cameron Dezfulian[1], Samuel M Poloyac[2], Edwin K Jackson[3], Robert SB Clark[1] and Patrick M Kochanek[1]

Splicing factors (SFs) coordinate nuclear intron/exon splicing of RNA. Splicing factor disturbances can cause cell death. RNA binding motif 5 (RBM5) and 10 (RBM10) promote apoptosis in cancer cells by activating detrimental alternative splicing of key death/survival genes. The role(s) of RBM5/10 in neurons has not been established. Here, we report that RBM5 knockdown in human neuronal cells decreases caspase activation by staurosporine. In contrast, RBM10 knockdown augments caspase activation. To determine whether brain injury alters RBM signaling, we measured RBM5/10 protein in mouse cortical/hippocampus homogenates after controlled cortical impact (CCI) traumatic brain injury (TBI) plus hemorrhagic shock (CCI+HS). The RBM5/10 staining was higher 48 to 72 hours after injury and appeared to be increased in neuronal nuclei of the hippocampus. We also measured levels of other nuclear SFs known to be essential for cellular viability and report that splicing factor 1 (SF1) but not splicing factor 3A (SF3A) decreased 4 to 72 hours after injury. Finally, we confirm that RBM5/10 regulate protein expression of several target genes including caspase-2, cellular FLICE-like inhibitory protein (c-FLIP), LETM1 Domain-Containing Protein 1 (LETMD1), and amyloid precursor-like protein 2 (APLP2) in neuronal cells. Knockdown of RBM5 appeared to increase expression of c-FLIP(s), LETMD1, and APLP2 but decrease caspase-2.

Journal of Cerebral Blood Flow & Metabolism (2015) **35,** 655–666; doi:10.1038/jcbfm.2014.242; published online 14 January 2015

Keywords: brain; neuron; RBM5; RBM10; splicing factors; traumatic brain injury

INTRODUCTION

Precursor messenger RNA (pre-mRNA) consists of exons (protein-coding RNA) and introns (noncoding RNA). Enzymatic intron removal by splicing mechanisms processes pre-mRNAs into mature mRNAs, which are then translated into protein. Genes that regulate cell death/survival are modified by alternative splicing.[1] Inclusion or exclusion of key coding exons generates different protein variants with altered function(s)—such as converting pro-death mediators into survival molecules or vice versa.[1,2] Alternative splicing and variant selection are regulated by hundreds of nuclear splicing factors (SFs) in the spliceosome.[3] Identifying SFs that promote expression of detrimental splice variants in neurons may lead to new treatments for brain injury.

The nuclear SFs RNA binding motif 5 (RBM5) and 10 (RBM10) regulate alternative splicing of cell death genes and promote apoptosis in some cancer cells.[4–7] RNA binding motif gene targets include caspase-2 and cellular FLICE-like inhibitory protein (c-FLIP). The protease caspase-2 has a long variant caspase-2(L) that is pro-death but a short variant caspase-2(s) that is protective.[2,8] Cellular FLICE-like inhibitory proteins are mostly protective but the long variant c-FLIP(L) is less potent than shorter c-FLIP(s).[9–11] RNA binding motif 5 increases caspase-2(L) and c-FLIP(L) splicing, which favors cell death.[4,12] Overexpression of RBM5/10 greatly sensitizes cancer cells to die by death ligands such as tumor necrosis factor alpha (TNF-*α*) that induce caspase-mediated apoptosis.[13,14] It is unclear whether RBM5/10 regulate maladaptive splicing and caspase activation after injury in neurons.

Few studies have investigated intron/exon splicing changes after acute central nervous system injury like traumatic brain injury (TBI). Traumatic brain injury is a major cause of death and disability. Secondary insults such as hypotension from hemorrhage (H) or hemorrhagic shock (HS) greatly increase mortality and morbidity in TBI patients.[15] It also increases neuronal death by exacerbating secondary hypoxia-ischemia in injured brain regions in animal models.[16] To the best of our knowledge, SF changes have not been investigated in TBI. Confirmation of SF disturbances in TBI could help to clarify the relevance of this understudied signaling axis in central nervous system therapeutics. We measured protein levels of RBM5, RBM10, splicing factor 1 (SF1), and splicing factor 3A (SF3A) in brain tissue homogenates 4, 24, 48, and 72 hours after combined controlled cortical impact plus HS (CCI+HS) in mice. We included SF1 and SF3A in those studies because they are well-known master regulators of intron and exon splicing.

Here, we show that isolated neurons primarily express a 120-kDa RBM5 protein. Knockdown of neuronal RBM5 inhibited

[1]Department of Critical Care Medicine, Safar Center for Resuscitation Research, University of Pittsburgh School of Medicine, Pittsburgh, Pennsylvania, USA; [2]Pharmaceutical Sciences Department, University of Pittsburgh School of Pharmacy, Pittsburgh, Pennsylvania, USA and [3]Department of Pharmacology and Chemical Biology, University of Pittsburgh School of Medicine, Pittsburgh, Pennsylvania, USA. Correspondence: Dr TC Jackson, Department of Critical Care Medicine, Safar Center for Resuscitation Research, University of Pittsburgh School of Medicine, 3434 Fifth Avenue, Pittsburgh 15260 PA, USA.
E-mail: jacksontc@upmc.edu
This work was supported by NIH/NINDS grant 1R21NS088145 to TCJ, US Army grant W81XWH-10-1-0623 to PMK, and NIH/NINDS grant R01NS087978 to PMK and EKJ.
Received 2 September 2014; revised 6 November 2014; accepted 8 December 2014; published online 14 January 2015

staurosporine (STS)-induced caspase activation, and altered protein expression of survival/death genes. A 90- kDa RBM5 protein was additionally observed in whole brain tissue extracts. The 90-kDa RBM5 protein decreased after CCI+HS. In contrast, RBM5 staining appeared greater in nuclei of hippocampal neurons after CCI+HS —suggesting that neuronal RBM5 is upregulated in select brain regions after injury. Anti-RBM10 antibody detected a 100/120-kDa double band in isolated neurons and whole brain tissue extracts, and increased after CCI+HS. Neuronal RBM10 knockdown exacerbated STS-induced caspase activation revealing potential antiapoptotic functions. Finally, SF1 protein decreased after CCI+HS.

MATERIALS AND METHODS

Chemicals and Reagents

Retinoic acid (RA) was purchased from SIGMA (St Louis, MO, USA). Dimethyl sulfoxide (DMSO) was purchased from SIGMA. Hematoxylin and Eosin Y (H&E) stains were purchased from Thermo Fisher-Shandon (Pittsburgh, PA, USA). Fluorojade B (FJB) was purchased from Chemicon (Temecula, CA, USA). Primary antibodies were purchased from: Anti-RBM5 (Atlas Antibodies, Stockholm, Sweden; Cat#HPA018011, Lot#R07119), Anti-RBM10 (purchased via Sigma but generated by Atlas Antibodies; Cat# HPA034972, Lost#R32333), Anti-SF1 (Atlas Antibodies; Cat#HPA018883, Lot#R07869), Anti-SF3A subunit 1 (purchased via Sigma but generated by Atlas Antibodies; Cat#HPA000690, Lot#R00090) Anti-c-$FLIP_{L/S}$ (H-202) (Santa Cruz, Dallas, TX, USA; Cat#sc-8347, Lot#J2010), Caspase-$2_{L/S}$ (BD Biosciences/Pharmingen, San Jose, CA, USA; Cat#51-1395GR), Anti-TNF-α (TNF-α; Cell Signaling Technology, Danvers, MA, USA; Cat#3707), Anti-Poly ADP ribose polymerase (PARP) Total/cleaved (Cell Signaling Technology; Cat#9532), Anti-Caspase-9 Total/cleaved (Cell Signaling Technology; Cat#9502), Anti-Caspase Cleavage Products (Cell Signaling Technology; Cat#8698), Anti-α-Fodrin (Enzo Life Sciences, Farmingdale, NY, USA; Cat#BML-FG6090-0500, Lot#08231207), Anti-LETM1 Domain-Containing Protein 1 (LETMD1; Lifespan Biosciences, Seattle, WA, USA; Cat# LS-C116277), Anti-amyloid precursor-like protein 2 (APLP2; purchased via Sigma but generated by Atlas Antibodies; Cat# HPA039319, Lost#R326082), Anti-α-Tubulin (Cell Signaling Technology; Cat#2144). Goat anti-rabbit and goat anti-mouse secondary antibodies were purchased from Life Technologies (Grand Island, NY, USA).

Animals

All animal work was approved by the Institutional Animal Care and Use Committee of the University of Pittsburgh. Protocols follow recommendations established by the American Medical Veterinary Association Guideline for Euthanasia. Studies were designed to minimize pain and suffering, and to use the minimum number of animals required to achieve significance. Animals were granted *ab libitum* accesses to food and water. All animals were maintained on 12 hours light/dark cycle.

Traumatic Brain Injury Mouse Model

In all, 12- to 15-week-old male C57BL/6 mice (Jackson Laboratories, Bar Harbor, ME, USA) were used for CCI+HS. Mice were injured by CCI+HS as described by our group.[16] *CCI injury:* Briefly, anesthesia was initiated by 4% isoflurane in 70% N_2O/30% O_2. Animals securely placed inside a stereotaxic frame were positioned under isoflurane nose-cone. Isoflurane was reduced to 2% for maintenance anesthesia. Body temperature recorded via a rectal probe, and catheters inserted into the left femoral artery and vein. The head was shaved, sterilized with betadine, and skin opened. A craniotomy over the left parietal cortex was introduced via a dental drill. A pressure-driven pneumatic impactor, with a 3-mm steel flat tip, was applied to the brain for CCI. The magnitude of injury is controlled by impact velocity and depth of tip penetration into the brain. Mild-moderate CCI (velocity 5/ms; depth 1.0 mm) was employed for combined injury experiments. *Combined hemorrhagic shock:* 5 minutes after CCI, isoflurane was reduced to 0.5%, and blood removed via femoral vein connected to a syringe containing citrate anticoagulant. Blood was withdrawn over 15 minutes until mean arterial blood pressure (MABP) reached 25 to 27 mm Hg in mice. Shock was maintained 35 minutes by either removing or readministering shed blood in 50 μL aliquots (to clamp target MABP). After HS, mice were volume resuscitated using 20 mL/kg lactated ringers. Target MABP during the 90-minutes 'Pre-Hospital Care Phase' was 70 mm Hg. Additional 10 mL/kg aliquots of lactated ringers were administered over 90 minutes if required to maintain target MABP. Finally, a 'Hospital Phase' was initiated by returning shed blood to mice over 15 minutes. Blood pressure normally returns to baseline levels (~90 mm Hg). Mice were allowed to recover after CCI+HS injury (weaned from isoflurane and catheters removed). Finally, mice were given supplemental oxygen 30 minutes before return to animal housing for stability. Naïve mice were not exposed to experimental manipulations. Sham mice received craniotomy and catheterization but neither CCI nor HS. Mice were randomized to sham/injury and killing timepoint. Naïve mice were not randomized. For biochemistry studies, mice were killed 4, 24, 48, and 72 hours after injury, tissues snap-frozen in liquid nitrogen, and stored at − 80°C until homogenization in radioimmunoprecipitation assay (RIPA) buffer. For immunohistochemistry/staining studies, mice were anesthetized, killed at 48 hours by transcardially perfusing with saline followed by 10% formalin, and brains collected for subsequent processing with antibodies, FJB staining, or H&E staining as previously described by our group.[16] Investigators were not blinded to injury groups.

Primary Cortical Neuron Culture

Cortical neuron cultures were prepared as reported by our group.[17] Briefly, embryos were isolated from timed pregnant (E16 to 18) Sprague Dawley (SD; Charles River, Wilmington, MA, USA) rats. Minced cortical tissue transferred into a 15-mL tube and spun at 5 minutes/200 *g*/4°C. Tissue was trypsinized 8 minutes at 37°C, triturated (1% DNAse in Hanks Balanced Salt Solution) 10 times through a fire-polished glass Pasteur pipette, and resuspended in Neurobasal/B27 (Life Technologies). Neurobasal Media/B27 plating media was supplemented with 25 μM Glutamic Acid, Pen-Strep, and L-Glutamine. Neurons were counted on a hemacytometer and seeded onto 8-well glass slides or 6-well plates (~2 to 4×10^5 and ~ 1 to 2×10^6, respectively). Half the media was replaced every 3 to 4 days with fresh Neurobasal Media/B27 (minus Glutamic Acid). The mitotic inhibitor cytosine β-D-arabinofuranoside hydrochloride (ARA-C; SIGMA) was added to 6-well plates on day *in vitro* (DIV) 3 to prevent glial proliferation and maintain pure neuron cultures for western blot biochemistry experiments. For immunofluorescence studies, glass culture slides were coated overnight with 50 μg/mL Poly-D-Lysine (SIGMA), washed twice with sterile ddH_2O, and air dried in a laminar flow hood. Astrocytes were allowed to proliferate by not including ARA-C. At DIV 12, slides were washed with PBS, fixed in 4% paraformaldehyde for 25 minutes, membranes permeated with 0.1% Triton X-100/PBS for 15 minutes, washed and blocked in 1% bovine serum albumin/20%goat serum/PBS for ~ 1 hour. Primary antibodies were diluted in 3% goat serum/PBS and incubated on glass slides overnight at 4°C. Cells were washed, incubated with secondary antibodies (Alexa Fluor Goat-anti Rabbit 594 and Alexa Fluor Goat-anti mouse 488 (Life Technologies) for 1.5 hours, washed, mounted in ProLong Gold Antifade with DAPI (Life Technologies), and imaged on a fluorescent microscope (Eclipse 50 Nikon, Melville, NY, USA).

Lentivirus Transduction and Differentiation of Human Neuronal SHSY5Y Cells

Human SHSY5Y cells were purchased from ATCC (Manassas, VA, USA). Lentivirus work was approved by the Institutional Biosafety Committee of the University of Pittsburgh. Pre-made BSL-2 lentivirus aliquots containing 200 μL of 1×10^6 infectious particles were purchased from Santa Cruz Biotechnology (Dallas, TX, USA), including nontargeting (NT) shRNAs; Cat#sc-108080, RBM5 targeting shRNAs; Cat#sc-10674-V1, and RBM10 targeting shRNAs; Cat#sc-76362-V. Undifferentiated SHSY5Ys were maintained in Opti-MEM culture media (Life Technologies) supplemented with 10% FBS (GE Healthcare Life Sciences, HyClone Laboratories, Logan, UT, USA). Cells were seeded onto small T-12.5 cm flasks. Twenty-four hours later at ~50% confluence SHSY5Ys were transduced with lentivirus (1 flask per each group). Transduction media consisted of 50 μL virus+2 μg/mL Polybrene (Santa Cruz) in 2 mL of growth media. Seventy-two hours after start of transduction, cells were washed twice with basal Opti-MEM (no FBS), trypsinized for ~2 minutes (0.05% Trypsin/EDTA; Life Technologies), protease activity quenched in growth media, centrifuged 5 minutes/200 *g*/4°C, resuspended in fresh growth media, and seeded onto 75 cm^2 sterile flasks (same protocol used for all subsequent propagations). Forty-eight hours later, cultures received fresh growth media containing 1 μg/mL puromycin dihydrochloride (Santa Cruz). Lentiviral expression plasmids contain a puromycin resistance gene. Cells not transduced by lentivirus are killed by puromycin. Pilot dose-death experiments found that 1 μg/mL puromycin killed >90% nontransduced SHSY5Ys by 48 to 72 hours. For the first 3 selection days, media was replaced each day to remove debris. At confluence, they were again propagated into new 75 cm^2 and 225 cm^2 sterile flasks and selected 3 more days (6 days total puromycin selection). Thawed cryogenically stored NT and RBM knockdown cells were subjected to an additional 3 to 4 extra days of puromycin selection in preparation for different downstream experiments. Puromycin selection was discontinued a minimum of 3 days before experimentation in all studies. Cells were counted using a Cellometer (Nexcelom Bioscience, Lawrence, MA, USA). In all, 1×10^6 cells/well were seeded onto four individual 6-well plates ($n = 2$ replicates in each group per plate). Undifferentiated cells were harvested in RIPA buffer 24 hours later (two plates or $n = 4$ replicates/group). The remaining two plates were differentiated. Growth media was replaced with differentiation media (Opti-MEM/1%FBS/10 μM RA). Retinoic acid was dissolved in 100% DMSO, aliquoted into sterile vials, and stored at −80°C in a light-sealed box. Retinoic acid was directly added to media at final concentration. Final DMSO concentrations were 0.04%. Differentiation conditions were maintained by ½ media exchange every 2 days (with fresh RA). On differentiation day 7, human neuronal cells were harvested in RIPA buffer ($n = 4$ replicates/group). Cells were stored at −80°C for biochemistry. In neuronal death studies, media was replaced with basal Opti-MEM containing 150 nmol/L STS or equal volume DMSO control ($n = 6$ replicates/group). For immunofluorescence studies in undifferentiated SHSY5Ys, cells were seeded onto poly-D-lysine coated glass culture slides at a density of 80,000 cells/well, and processed the following day as described above for primary neurons.

Western Blot

As reported by our group,[17] tissues and cells were sonicated in RIPA buffer containing EDTA, protease inhibitors, and phosphatase inhibitors (Thermo Scientific-PIERCE, Rockford, IL, USA). Homogenized material was spun 10 minutes/16,000 *g*/4°C. Supernatants were collected for downstream SDS-PAGE. Protein quantification was determined by BCA assay (Thermo Scientific-PIERCE). In all, 10 to 20 μg protein was mixed with 2× or 4× Laemmli loading buffer (Bio-Rad, Hercules, CA, USA), heated to 95°C/5 minutes, and loaded onto 10- or 15-well pre-cast TGX 1% to 15% gradient gels (Bio-Rad). Gels were run at 150 V. Protein was transferred onto polyvinylidene fluoride membranes (GE Healthcare, Pittsburgh, PA, USA). Precision Plus Kaleidoscope protein standards (Bio-Rad) were included for molecular weight (MW) estimation. Membranes were washed 10 minutes in 1× Tris-Buffered saline (TBS; Bio-Rad). Traditional housekeeping gene loading controls showed variable changes after injury (Supplementary Figure 1). Staining is a more accurate method to control for protein loading in injured brain.[18,19] Therefore, densitometry of RBM5, RBM10, SF1, and SF3A was normalized to total protein stain in CCI+HS injury experiments (Supplementary Figure 2). Membranes were stained with reversible Swift Membrane Stain (Fisher Scientific, Waltham, MA, USA). Stained blots were saved to file using a flatbed scanner and analyzed by densitometry. Stain was quickly removed, membranes washed in TBS, and blocked 1 hour in TBS-Tween-20 (TBST)+7.5% blotting grade milk (TBS-T/milk). Primary antibodies were prepared in TBS-T/milk, and blots incubated overnight on a slow rocker at 4°C. Blots were washed 3×/5 minutes in TBS. Secondary antibodies were prepared in TBS-T/milk and incubated 2 hours on an orbital shaker. Blots were washed 3×/5 minutes in TBS, incubated ~2 minutes with ECL-2 HRP-detection reagent (Thermo Fisher-PIERECE), and membranes exposed to film in a dark room. Developed films were saved to file using a flatbed scanner, images compiled in Photoshop, and densitometry analyzed by UN-SCAN-IT software (Silk Scientific, Orem, UT, USA).

Immunohistochemistry and Tissue Staining

At 48 hours after injury, anesthetized mice were flushed with heparinized ice-cold saline by transcardial perfusion into the left ventricle. Tissues were immediately flushed with 10% buffered formalin. Brains removed and postfixed in 10% buffered formalin for 72 hours. Brains were cut into 3 mm coronal sections, dehydrated by serial alcohol preparations, cleared with Xylene, and embedded into paraffin wax. Coronal blocks were cut into 5 μmol/L sections via a microtome, and mounted onto glass slides. Avidin-biotin complex/3′,3′-Diaminobenzidine was used for visualization of RBMs by immunodetection. Briefly, deparaffinized tissue slides were subjected to antigen retrieval by heat-microwave in Antigen Decloaker solution (Biocare Medical, Concord, CA, USA). Slides were incubated 30 minutes in 3% H_2O_2/methanol to quench endogenous peroxidase activity. Slides were blocked 20 minutes in automation buffer containing 3% normal goat serum. Primary antibodies were diluted in 3% goat serum/buffer and incubated overnight at 4°C. Slides were washed and incubated 1 hour with biotinylated goat anti-rabbit IgG diluted in buffer (Vector Laboratories, Burlingame, CA, USA). Slides were washed, incubated 1 hour with Avidin-biotin complex reagent (Vector Laboratories), and treated with 3′,3′-Diaminobenzidine reagent (Vector Laboratories) for 5 to 10 minutes. Sections were counterstained with hematoxylin for 30 seconds. Slides were mounted with a coverslip and images collected on a Nikon Eclipse 90i microscope (Nikon). Hematoxylin and Eosin and FJB staining procedures were performed in CCI+H mice as reported by our group.[16] Sections were deparaffinized, treated with hematoxylin stain (Thermo Scientific, Waltham, MA, USA), washed, treated with Bluing reagent (Thermo Scientific), washed, and treated with Eosin Y (Thermo Scientific). Alternatively, sections were stained 30 minutes with FJB, washed, mounted, and imaged.

Statistical Analysis

Data were analyzed using the GraphPad PRISM software (GraphPad Software Inc., La Jolla, CA, USA). Multiple comparisons were analyzed by ANOVA and Newman-Keuls Multiple Comparison *post-hoc* analysis. Data were considered as significant at $P < 0.05$ using two-tailed tests. All graphs were created in GraphPad PRISM software and show mean+s.e.m. Experiments in which raw data of group comparisons were acquired as relative units (i.e., densitometry/pixel

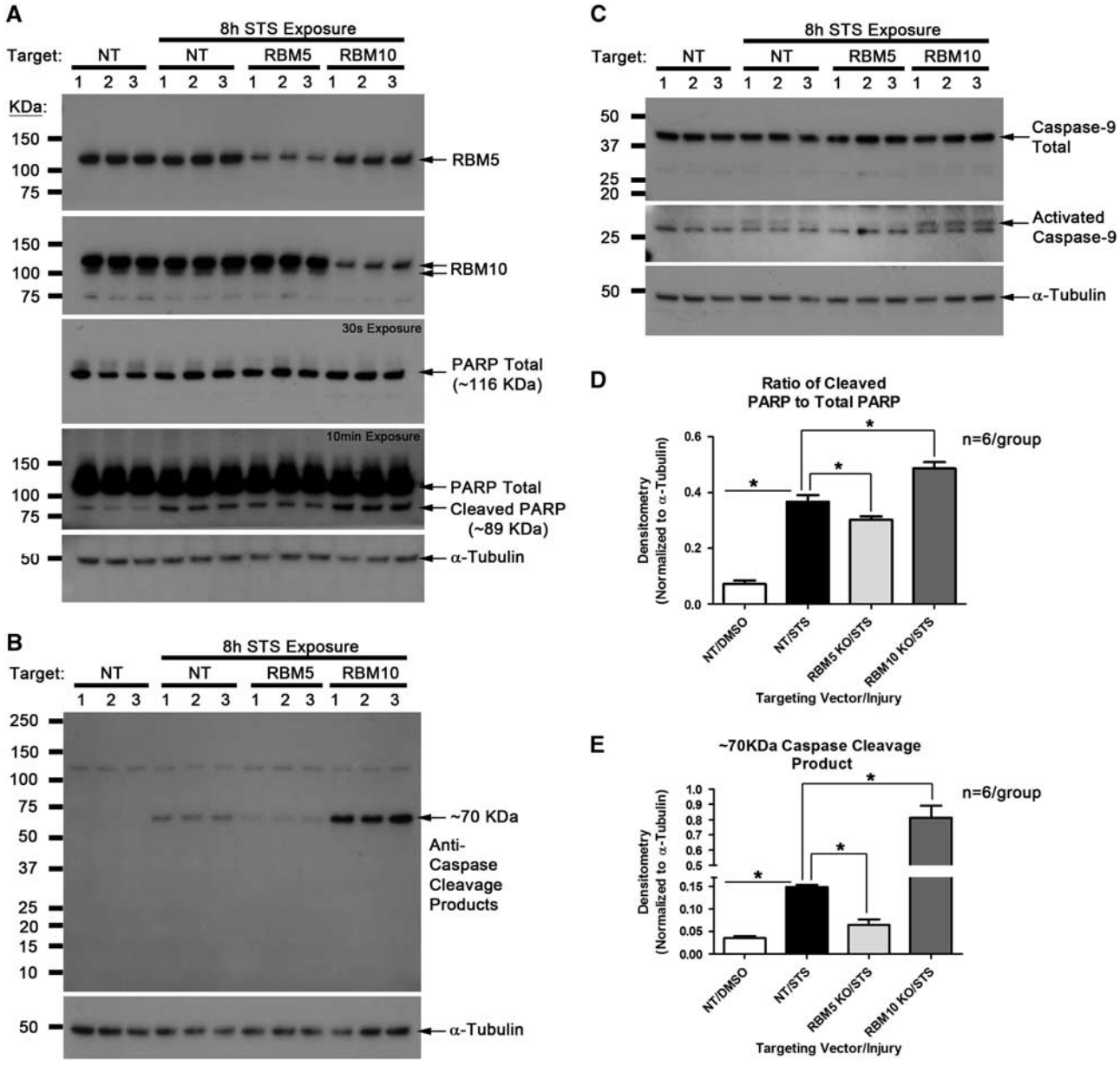

Figure 1. RNA binding motif 5 (RBM5) knockdown decreases staurosporine (STS)-induced caspase activation. Differentiated human neurons were subjected to 150 nmol/L STS injury for 8 hours. (**A** and **D**) 20 μg protein was loaded/well. Representative westerns ($n = 3$) confirm targeted knockdown of RBM5 or RBM10, and show effect of RBM inhibition of STS-induced apoptotic poly ADP ribose polymerase (PARP) cleavage. Densitometric semiquantitative analysis show a significant decrease in PARP total:cleavage ratio in RBM5 knockdown neurons versus nontargeting (NT) controls ($n = 6$/group; $P < 0.0001$). Results also show a significant increase in PARP cleavage in STS-treated RBM10 knockdown neurons ($n = 6$/group). (**B** and **E**) 20 μg protein was loaded/well. Representative westerns ($n = 3$) show effect of RBM inhibition on STS-induced apoptotic cleavage of a dominant ~70 kDa protein substrate. Densitometric semiquantitative analysis shows a significant decrease in the ~70-kDa STS-induced cleave product in RBM5 knockdown neurons versus NT controls ($n = 6$/group; $P < 0.0001$). Results also show a significant increase in the ~70-kDa STS induced cleave product in STS-treated RBM10 KD neurons ($n = 6$/group). (**C**) 20 μg protein was loaded/well. Consistent with PARP and ~70 kDa caspase cleaved product changes induced by gene knockdown in the presence of 8 hours STS, representative westerns ($n = 3$) show initiator caspase-9 activation is reduced in RBM5 knockdown cells but increased in RBM10 knockdown cells. Multiple comparisons were analyzed by one-way ANOVA and Newman-Keuls *post hoc*. Data were significant at $P < 0.05$. (*) indicates *post hoc* significant difference compared with NT controls. NS, not significant. Graphs show mean+s.e.m. Raw results of the (α-tubulin normalized) ~70 kDa cleavage product were transformed to Log(Y) values for statistical analysis.

intensity), data were standardized by expressing group differences as values between 0 and 1 (i.e., on the y axis). In Figure 7E, graphed densitometry data of caspase cleavage products normalized to α-tubulin were transformed to log(Y) values for statistical comparisons to correct for nonnormality in data distribution.

RESULTS

RNA Binding Motif 5 Regulates Caspase Activation and Protein Expression/Splicing in Neurons

Human neuronal SHSY5Ys were transduced with lentivirus to deliver NT control, RBM5 targeting, or RBM10 targeting

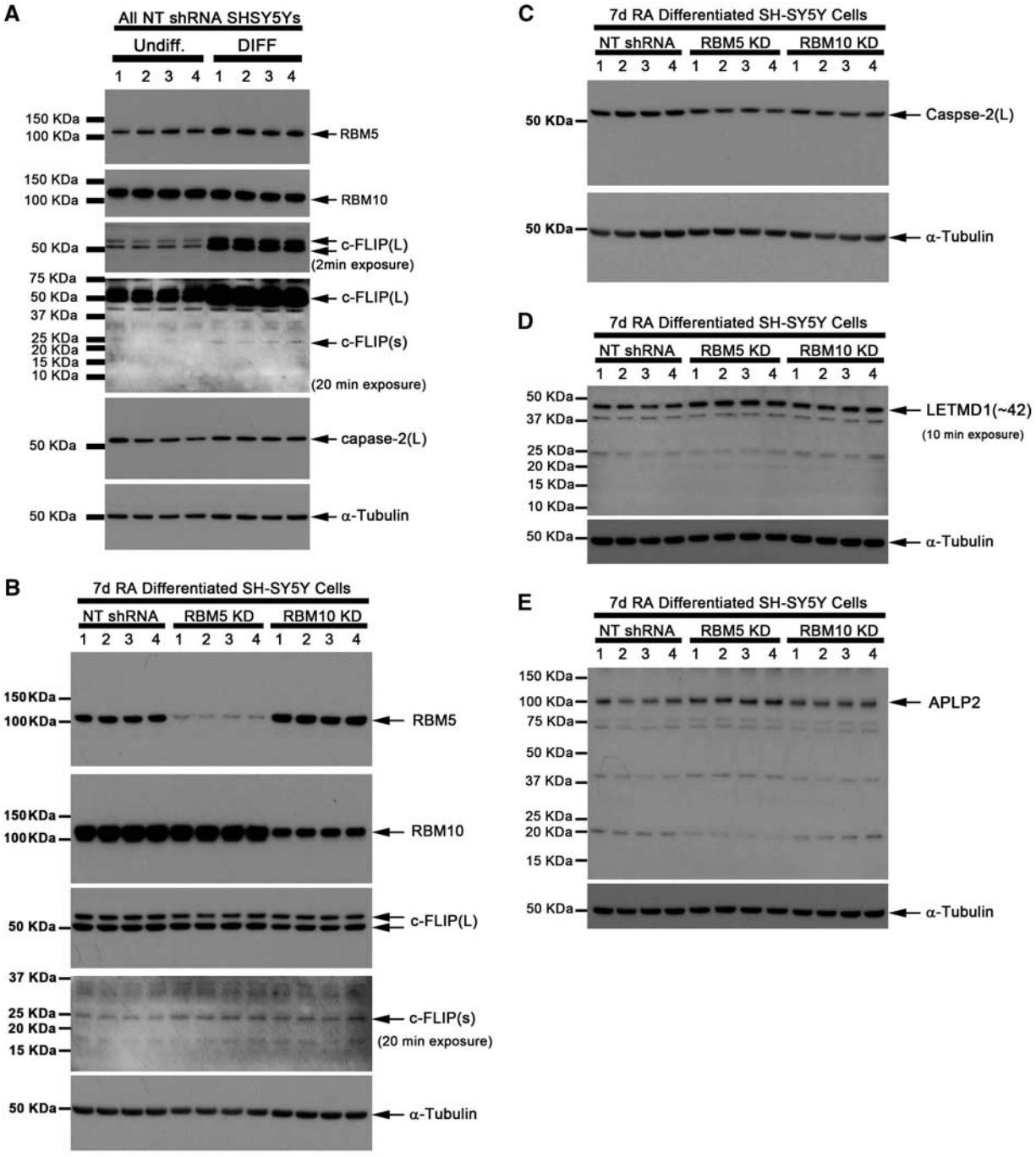

Figure 2. RNA binding motif 5 (RBM5) knockdown increases c-FLIP(s), LETM1 Domain-Containing Protein 1 (LETMD1), and APLP2 but decreases caspase-2(L) in human neuronal SHSY5Y cells. (**A**) 20 μg protein was loaded/well. Westerns show effect of 7days 10 μmol/L retinoic acid (RA) induced neuronal differentiation on RBMs, and their potential targets ($n = 3$/group). Differentiation (DIFF) appears to increase RBM5, c-FLIP(L), and c-FLIP(s). Levels for proteins of interest were compared in DIFF cells made to overexpress nontargeting (NT), RBM5, or RBM10 targeting shRNAs ($n = 4$/group). (**B**) 20 μg protein was loaded/well. Westerns show c-FLIP(s) levels appear increased in RBM5 knockdown neurons. (**C**) Westerns show caspase-2(L) levels appear decreased in RBM5 knockdown neurons. (**D**) Westerns show LETMD1 (predicted full-length protein ~42 kDa) appears increased in RBM5 and RBM10 knockdown neurons. (**E**) Westerns show APLP2 (predicted full-length protein ~87 kDa but observed as a 100- to 120-kDa band in brain[40]) appears increased in RBM5 knockdown neurons. c-FLIP,cellular FLICE-like inhibitory protein.

shRNAs. RNA binding motif 5 is a 92-kDA protein and reportedly migrates on SDS-PAGE at ~90 kDa but also commonly observed at ~120 kDa.[20] The ~120-kDa form of RBM5 was detected in SHSY5Ys, and decreased by knockdown (Supplementary Figure 3A). RNA binding motif 10 is a 103-kDa protein. Both an ~100-kDa and ~120-kDa RBM10 signal were detected in SHSY5Ys and decreased by knockdown (Supplementary Figure 3D).

Stably expressing/transduced SHSY5Ys cells were differentiated to neuronal phenotype by 7 days RA treatment. Neurons were

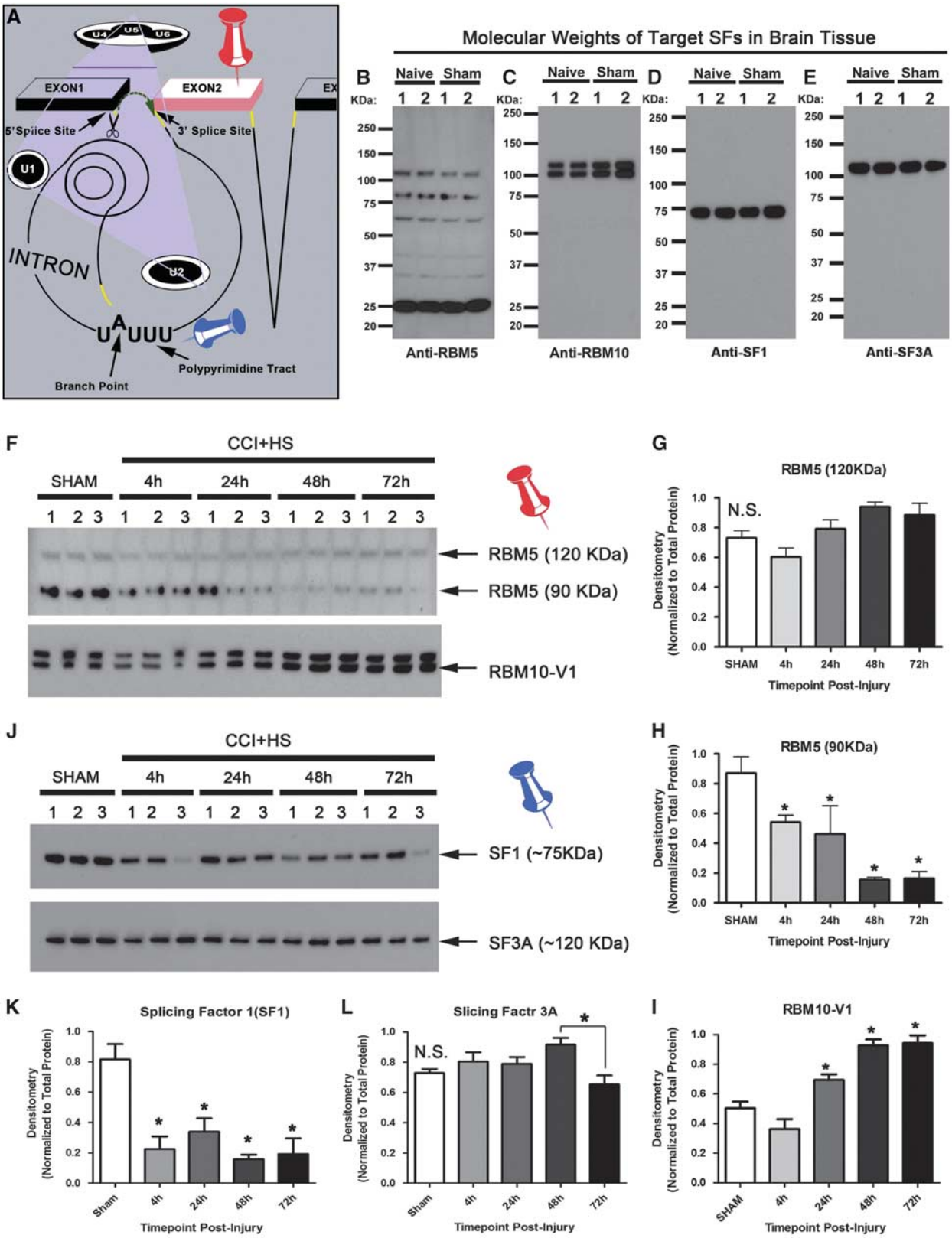

administered the caspase activator STS for 8 hours. Knockdown of RBM5 decreased PARP cleavage (Figures 1A and 1D), decreased caspase-9 activation (Figure 1C), and blocked cleavage of a major ~70 kDa caspase substrate (Figures 1B and 1E). Knockdown of RBM10 increased STS-induced caspase activation. It increased PARP cleavage (Figures 1A and 1D), increased caspase-9 activation (Figure1C), and increased cleavage of the ~70-kDa caspase substrate (Figures 1B and 1E).

Figure 3. Brain disturbances in splicing factor (SF) levels after CCI+HS. (**A**) Drawing illustrates SFs of interest and roles in the spliceosome. The fundamental spliceosome machinery is highlighted by the purple triangle (U complexes). Two ATP-dependent enzymatic splicing steps are required. The first step hydrolyzes the 5′splice site and ligates the intronic free-end to the internal branch point (BP). The second step (green arrow) ligates the end of exon 1 to beginning of exon 2, releasing intronic RNA. Hundreds of cofactors work to regulate the six key U-complex spliceosome components. RNA binding motif 5 (RBM5) and RBM10 (red pins) bind regions near the 3′ splice site of target exons. They destabilize U-complex interactions at target exons during the second splicing step (i.e., inhibit the green arrow). This causes the splicing machinery to bypass exon 2 and move to the next available 3′ splice site located at exon 3. Spliced exon 2, represented in pink, is then released as part of the flanking intronic material and exon1/exon3 are ligated together. SF1 and SF3A (blue pins) promote U2 complex binding to cis-acting elements near the BP—this is an essential early step in intron/exon splicing. Western blots show full molecular weight (MW) range and signals detected by antibodies against (**B**) RBM5, (**C**) RBM10, (**D**) SF1, and (**E**) SF3A large subunit in uninjured brains ($n = 2$ naïve and $n = 2$ sham). Ipsilateral cortical/hippocampal tissue homogenates were prepared from mice subjected to CCI+HS and collected at 4, 24, 48, and 72 hours after injury. Proteins were resolved on SDS-PAGE on 15-well gels (20 μg protein/well). Westerns show changes in (**F**) RBM5/ RBM10, and (**J**) SF1/SF3A. Graphs show densitometric semiquantification ($n = 3$/group) of (**G**) ~120 kDa RBM5 protein; $P = 0.0158$ (**H**) ~90 kDa RBM5; $P = 0.0029$, (**I**) ~100 kDa RBM10-V1; $P < 0.0001$, (**K**) ~75 kDa SF1; $P < 0.0015$, and (**L**) ~120 kDa SF3A; $P = 0.0369$. Data were analyzed by one-way ANOVA and Newman-Keuls *post hoc*. Data were significant at $P < 0.05$. (*) indicates *post hoc* significant difference compared with Sham. NS indicates *post hoc* comparison of shams versus injury groups and is not statistically different. Graphs show mean+s.e.m. CCI, controlled cortical impact; HS, hemorrhagic shock.

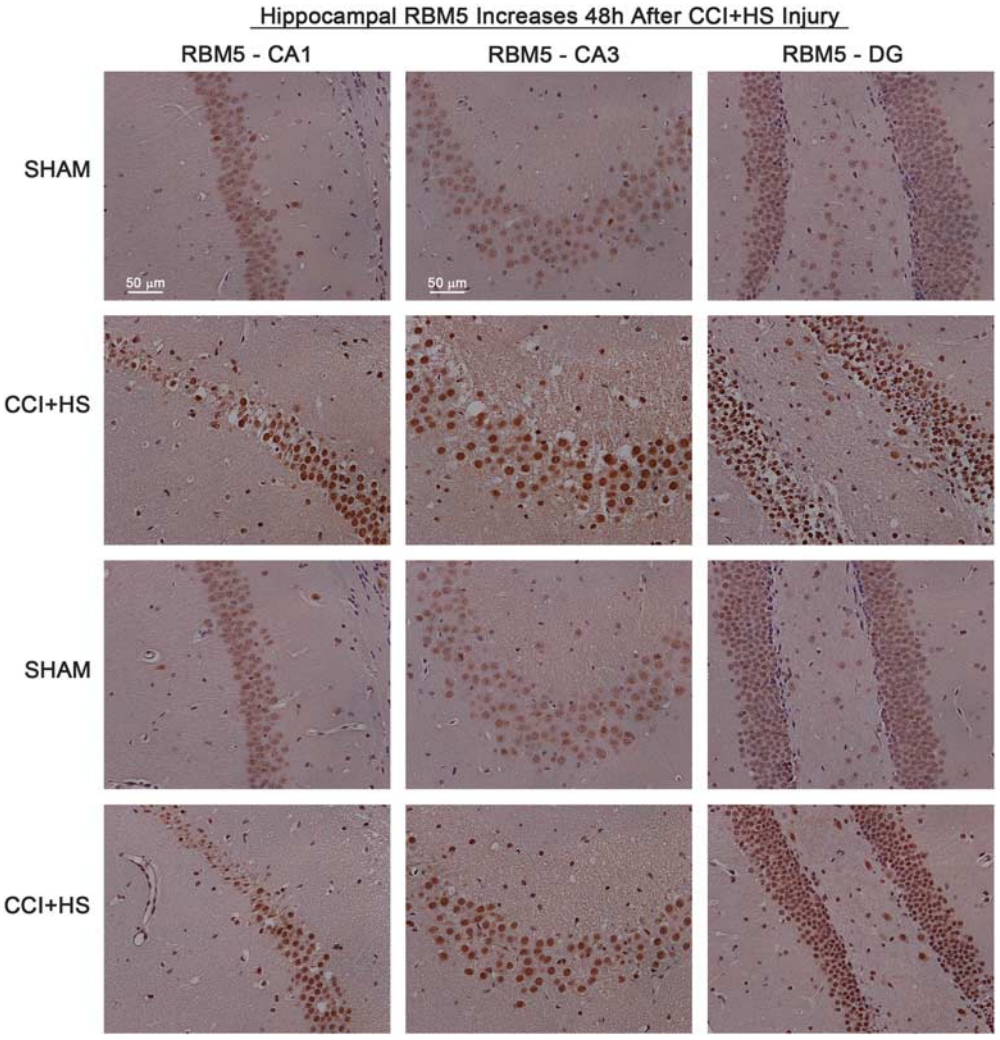

Figure 4. Increased RNA binding motif 5 (RBM5) staining in injured hippocampus. Brain tissue sections from sham ($n = 2$) and CCI+HS injured mice ($n = 2$) were collected 48 hours after injury and probed with antibody against RBM5. Immunohistochemistry shows ×20 magnification of CA1, CA3, and DG subregions. RBM5 staining (brown) is increased in all hippocampal regions of CCI+HS mice. CCI, controlled cortical impact; HS, hemorrhagic shock.

Cellular FLICE-like inhibitory protein and caspase-2 are known RBM5 splicing targets. We first measured whether the neuronal differentiation process affected protein variant expression of c-FLIP (L/s) and caspase-2 (L/s). Also, the c-FLIP and caspase-2 antibodies used in this experiment were reported to detect (L/s) splice variants in human cells.[8,21] Neuronal differentiation appeared to increase ~55 kDa c-FLIP(L) as well as ~26 kDa c-FLIP(s) variant (Figure 2A). Long exposure times required to observe c-FLIP(s)

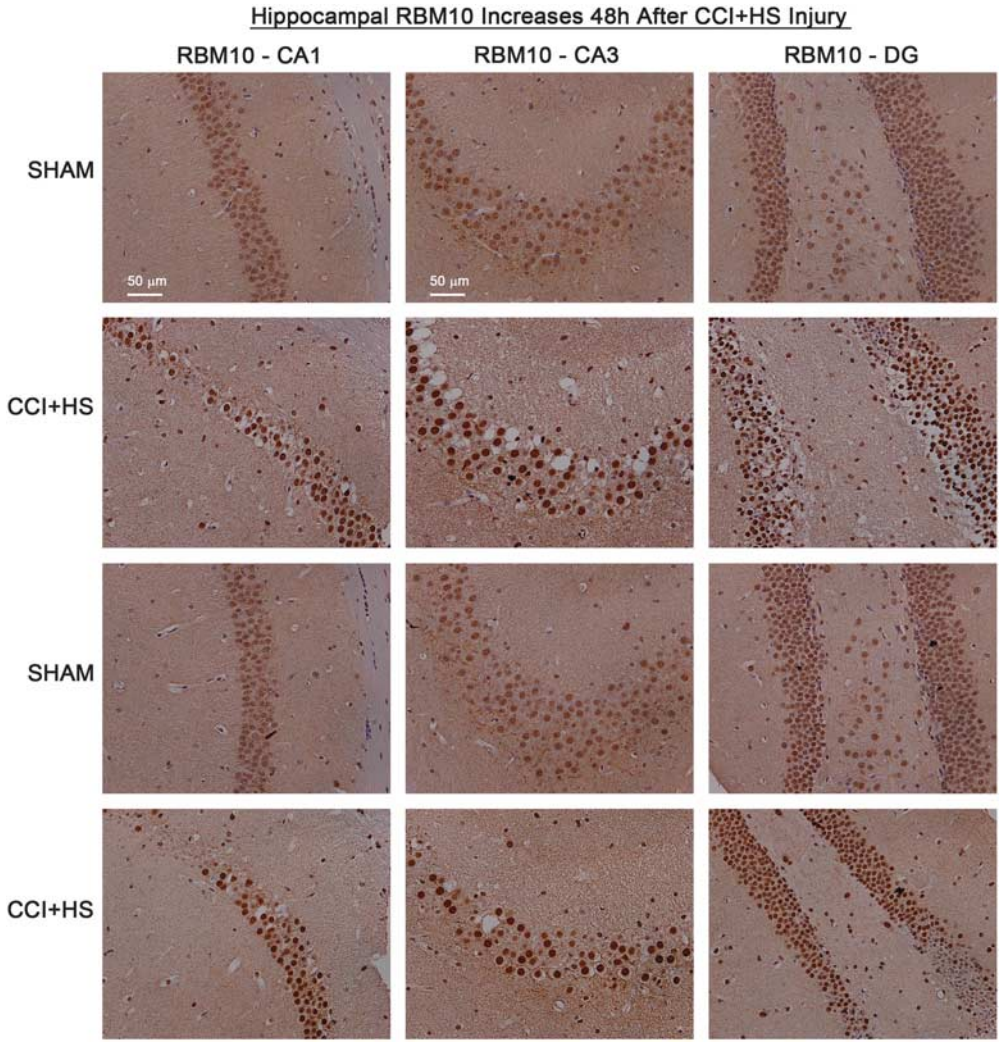

Figure 5. Increased RNA binding motif 10 (RBM10) staining in injured hippocampus. Brain tissue sections from sham ($n=2$) and CCI+HS injured mice ($n=2$) were collected 48 hours after injury and probed with antibody against RBM10. Immunohistochemistry shows $\times 20$ magnification of CA1, CA3, and DG subregions. RBM10 staining (brown) is increased in all hippocampal regions of CCI+HS mice. CCI, controlled cortical impact; HS, hemorrhagic shock.

protein are consistent with its high degradation rate relative to stable c-FLIP(L).[22] Only the caspase-2(L) variant was present in neurons (Figure 2A).

The effect of RBM5 or RBM10 knockdown on c-FLIP and caspase-2 expression/splicing in differentiated neurons was studied. Knockdown of RBM5 appeared to increase c-FLIP(s) but decrease caspase-2(L) protein levels (Figures 2B and 2C). Caspase-2(s) was not detected in any groups/treatments. We also measured levels of anti-apoptotic protein LETMD1, and levels of neuron development regulator APLP2—both reportedly RBM10 splicing targets. Knockdown of RBM5 and RBM10 appeared to increase LETMD1 protein in neurons (Figure 2D). Knockdown of RBM5 appeared to increase APLP2 (Figure 2E).

Splicing Factor Disturbances after Traumatic Brain Injury in Mice

Figure 3A illustrates SFs of interest (RBM5, RBM10, SF1, and SF3A) and summarizes their known roles in RNA splicing. We first characterized specificity of antibodies to detect SFs in brain. Consistent with prior reports using custom generated antibodies to detect RBM5,[20] we observed multiple signals across the MW range including an ~90-kDa and ~120-kDa product (Figure 3B). Of note, we tested several commercially available antibodies and only the anti-RBM5 antibody made by Atlas Antibodies detected RBM5 in our hands. We observed ~100 kDa (i.e., RBM10 variant 1; RBM10-V1) and ~120 kDa bands across the MW range in brain (Figure 3C). Splicing factor 1 encodes an ~75 kDa protein and the only signal detected in brain (Figure 3D). The large subunit of the SF3A complex is ~120 kDa and the only signal observed in brain (Figure 3E).

We next tested whether SFs are disturbed in the acute/subacute phase after CCI+HS—a brain injury model to maximize secondary neuronal death in TBI.[16] Splicing factors dynamically altered after brain injury. In all, ~120 kD RBM5 did not increase after injury compared with sham levels (Figures 3F and 3G) but was a larger component of the total RBM5 protein pool at later time points (Supplementary Figure 4B). In contrast, ~90 kDa RBM5 decreased after injury (Figures 3F and 3H). RBM10-V1 significantly increased by 24 hours after injury compared with shams (Figure 3F), and doubled by 48 to 72 hours after injury (Figure 3I). The higher migrating ~120 kDa RBM10 band was significantly higher by 48 hours after injury (Supplementary Figure 4C). Caspase cleavage

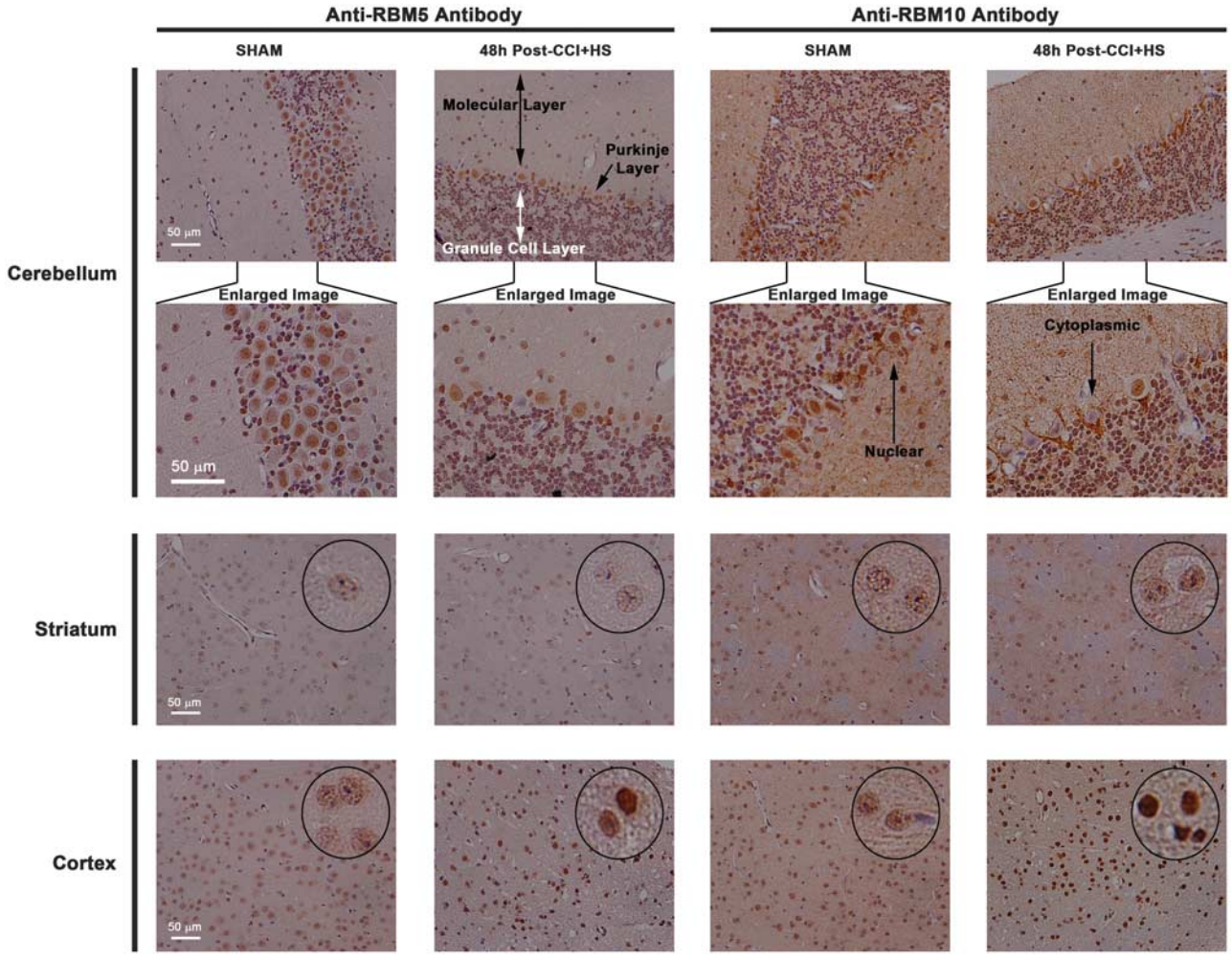

Figure 6. Increased RNA binding motif 5 (RBM5)/10 staining in injured cortex but not in ipsilateral striatum or cerebellum. Brain tissue sections of a sham and CCI+HS injured mouse at 48 hours after injury were probed with antibodies against RBM5 and RBM10 (×20 magnification). Cerebellar images at top (first row across) show representative pictures for injury group/RBM target. Cerebellar areas of interest were magnified in Photoshop (second row across) to highlight nuclear/cytoplasmic differences of RBM10 staining in some cerebellar neurons. Injury did not affect faint RBM staining in striatal neurons (third row across). Injury increased RBM staining in cortical neurons (fourth row across). Black circles show randomly selected neurons within each image field that were magnified in Photoshop to show speckled staining pattern.

products also increased by 48 hours after injury (Supplementary Figures 5G and 5H). Splicing factor 1 levels were significantly low at each time point postinjury compared with sham (Figures 3J and 3K). Splicing factor 3A levels did not differ from shams after injury but 48-hour levels were slightly increased relative to the 72-hour time point (Figure 3L).

We focused immunohistochemistry studies on RBM5 and RBM10 at 48 hours after injury because both increased by this time point. Levels of RBM5 appeared to increase in subfield neurons of the hippocampus 48 hours after injury (CA1, CA3, and DG; Figure 4). RNA binding motif 10 staining showed similar changes in the hippocampus (Figure 5). RNA binding motifs also appeared to increase in some cortical neuron populations but not striatal or cerebellum neurons (Figure 6). Circled cells in cortex/striatum show magnified fields of view from background images —the speckled pattern of RBM staining in nuclei of shams is consistent with spliceosomal regulators.[23] Also, RBM10 staining in some Purkinje neurons of the cerebellum seemed to favor cytoplasmic versus nuclear localization (Figure 6—black arrows in RBM10 cerebellum panels).

RNA binding motif staining in mouse tissues appeared highly neuronal and restricted to nuclei. To confirm this observation, we performed colocalization studies using primary rat cortical neurons. Day *in vitro* 12 neurons were probed with antibodies against RBM5/10 and signals colocalized with neurons and astrocytes. RBM5/RBM10 (RED) almost exclusively stained neurons (RBM5; Figures 7A to 7C; RBM10; Figures 7G to 7I). Little staining was observed in astrocytes (RBM5; Figures 7D to 7F; RBM10; Figures 7J to 7L). RNA binding motif 5/10 staining was restricted to nuclei and colocalized with DAPI (RBM5; Figures 7B and 7E; RBM10; Figures 7H and 7K). Protein homogenates were prepared from DIV 10 pure rat cortical neurons (i.e., ARA-c added to inhibit glial proliferation) and probed with antibodies against RBM5/10. The ~120-kDa RBM5 signal was the only band detected in primary rat cortical neurons (Figure 7M). Both the ~100-kDa and ~120-kDa RBM10 bands were detected (Figure 7N).

DISCUSSION

RNA Binding Motif 5 and RNA Binding Motif 10 Regulate Cell Death Biochemistry in Neurons

Caspase-2 and c-FLIP regulate neuronal death/survival.[24–26] Both genes encode multiple protein splice variants with different effects on cell death. The caspase-2(L) variant is toxic but caspase-2(s) is

protective. Cellular FLICE-like inhibitory protein is mostly protective but c-FLIP(s) is more potent than c-FLIP(L). No therapy currently exists to selectively upregulate protective splice variants.

The splicing factor RBM5 is abundant in reproductive organs and brain relative to other tissues.[27] RNA binding motif 5 may be a potential target to enhance pro-survival splicing of select genes including caspase-2 and c-FLIP. In cancer cells, RBM5 inhibition increases protective caspase-2(s) and c-FLIP(s) levels. However, it is unknown whether RBM5 also regulates splicing and/or promotes cell death in neurons. Here, we show that lentivirus/shRNA knockdown of RBM5 appears to increases c-FLIP(s), and reduce caspase-2(L) in human neuronal cells. Our results are consistent with findings by others in cancer cells. We did not observe an increase in caspase-2(s). Caspase-2(s) reportedly exists as a transient mRNA species and subject to rapid nonsense mediated decay.[28] Thus, it may not be a major effector of neuron survival—our results seem to support this idea because caspase-2(s) protein was undetectable in SHSY5Ys. To test the functional effect of protein changes on survival, we treated RBM knockdown neurons with caspase activator STS. As predicted, RBM5 inhibition decreased caspase activation. Surprisingly, RBM10 inhibition increased STS-induced caspase activation. Results confirm that RBM5 promotes caspase activation and pro-death splicing in neurons. Finally, RBM5 knockdown also increased APLP2—a key protein involved in cortical neuron development and synaptic function in adult mice.[29–31] This novel finding suggests that RBM5 may also regulate genes involved in neuronal function.

Inhibition of RBM10 did not increase c-FLIP or caspase-2 proteins in SHSY5Ys. This finding is supported by others. Inoue *et al*[5] report that RBM10 knockdown did not alter c-FLIP nor caspase-2 splicing in HeLa cells.[5] Furthermore, a recent (2013) study reported that RBM10 knockdown in human embryonic kidney 293 (HEK293) cells caused 304 mRNA exon splicing changes (256 inclusion events and 48 exclusion events).[32] Caspase-2 and c-FLIP were not reported as gene targets in those studies. However, LETMD1 and APLP2 were RBM10 gene targets—prompting us to examine them here. We confirm that inhibition of RBM10 or RBM5 appears to upregulate LETMD1 expression in SHSY5Ys. LETM1 Domain-Containing Protein 1 may be neuroprotective because it protects cells from UV and STS induced death.[33]

Prior studies suggest RBM5 and RBM10 have compensatory regulation (Supplementary Tables 3 and 4 in study by Wang *et al*[32]). Our findings agree with those observations. Knockdown of RBM10 in SHSY5Ys significantly raised RBM5 levels (Supplementary Figures 3A and C). Furthermore, decreased RBM5 levels correlate with increased RBM10 in sham versus injured mouse brain homogenates (Supplementary Figure 4A).

Exon Splicing Factors RNA Binding Motif 5 and RNA Binding Motif 10 are Disturbed after Traumatic Brain Injury

We predicted that SF disturbances might occur after TBI. Here, we report that RBM5/10 increase in hippocampus and cortex 48 hours after CCI+HS. Increased RBM levels coincide with neuronal degeneration (FJB), and neuronal loss (H&E) in hippocampus (Supplementary Figure 6; Figure 7). In addition, TNF-*α*, caspase cleaved *α*-Fodrin, and caspase cleavage products increased after CCI+HS (Supplementary Figure 5). Previous studies in cancer cells show that RBM5/10 overexpression sensitizes cells to TNF-*α* induced death and caspase activation (as well as the death ligands

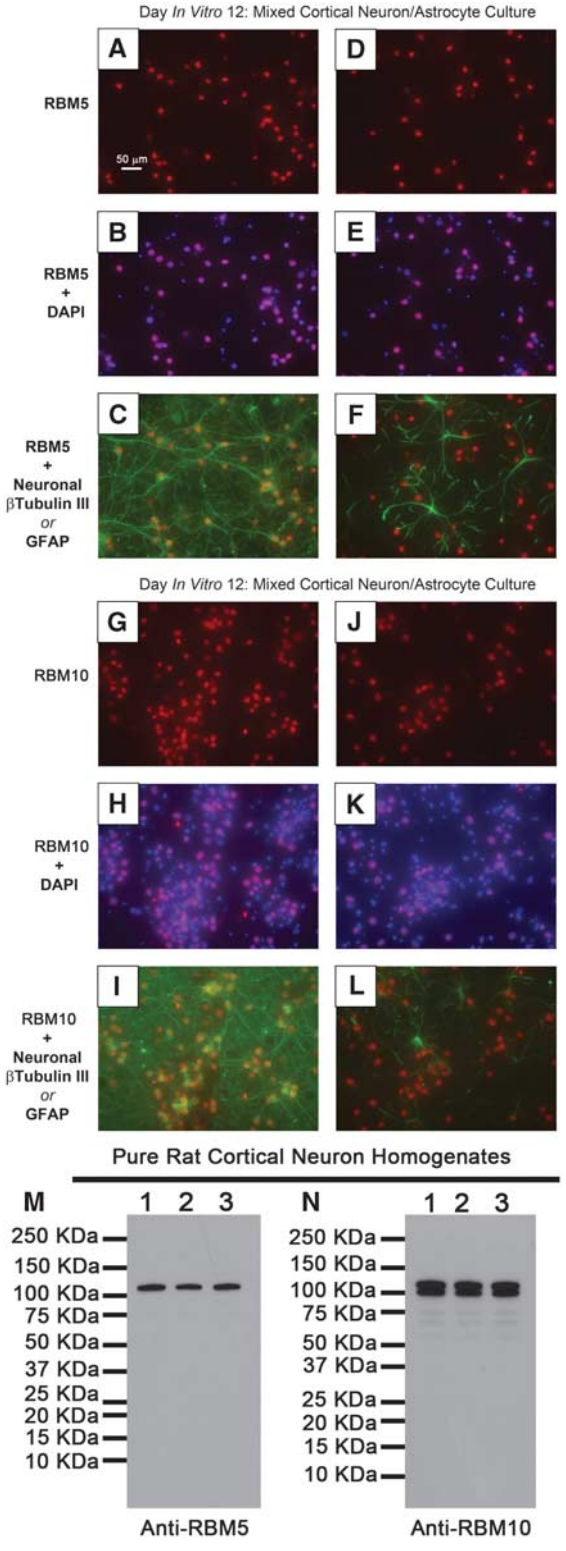

Figure 7. Characterization of RNA binding motif 5 (RBM5)/10 in cultured primary cortical neurons. Day *in vitro* (DIV) 12 mixed cortical neuron/astrocyte cultures were prepared for immunofluorescence. Images show ×40 magnification of (**A–F**) RBM5 and (**F**, **G**) RBM10 distribution. (**B**, **E**, **H**, **K**) RBM5/10 (RED) was mostly restricted to nuclei as shown by DAPI overlay. RBM5/10 (RED), almost exclusively colocalized with (**C** and **I**) the neuron-specific marker *β*-Tubulin III (GREEN) but not with (**F** and **L**) the astrocyte marker GFAP. Protein homogenates were prepared from DIV 10-enriched cortical neuron cultures to analyze RBM5/10 western signals specifically in neurons. (**M**) The ~120-kDa RBM5 signal was the only band detected in primary neuron homogenates. (**N**) The ~100-kDa and ~120-kDa RBM10 signals were detected in primary neuron homogenates.

TNF-related apoptosis-inducing ligand and Fas ligand). Here, we confirm that RBM5 promotes caspase activation in neuronal cells. It is possible that increased RBM5 in brain similarly sensitizes hippocampal/cortical neurons to die by extracellular TNF-*α* and other death ligands after injury. Future studies should examine whether RBM5 overexpression in primary rat cortical neurons sensitizes them to die by treatment with TNF-*α*, TNF-related apoptosis-inducing ligand, and Fas ligand. Alternatively, increased RBM10 may represent an endogenous neuroprotective response but again this hypothesis needs to be challenged by overexpression studies in primary neurons.

Western analysis of brain tissue homogenates show temporal changes of RBM5 proteins after injury. The calculated MW of RBM5 is 92 kDa. Approximately 90 kDa RBM5 decreased by 48 hours after injury. Approximately 120 kDa RBM5 levels did not differ in shams versus injury. However, the ratio of ~120 kDa/~90 kDa increased postTBI (Supplementary Figure 4B). Also, RBM5 staining appeared greater in neurons of the injured hippocampus—potentially revealing increased expression of neuronal RBM5 in select brain regions. Western analysis failed to detect IHC-like changes. This may be due to nonneuronal sources of ~120 kDa RBM5 diluting neuron-specific effects in whole tissue extracts. Consistent with the idea that neuronal RBM5 staining is detecting the ~120-kDa protein, immunofluorescence studies in SHSY5Ys show that differences in nuclear RBM5 staining match protein changes after knockdown (i.e., protein and IF signal appear to be reduced in RBM5 knockdown cells but increased in RBM10 knockdown cells; Supplementary Figure 3). Future studies need to compare RBM5 protein levels in culture homogenates from neurons, astrocytes, oligodendrocytes, microglia, pericytes, and brain endothelial cells. Sutherland *et al*[20] suggest that both ~90 kDa and ~120 kDa forms of RBM5 are linked to cell death. Results from SHSY5Y studies suggest that ~120 kDa RBM5 promotes cell death in neurons but the role of ~90 kDa RBM5 is still unclear. The calculated MW of RBM10-V1 is 103 kDa. The ~100-kDa and ~120-kDa forms of RBM10 increase after injury in hippocampus and cortex. Both signals are readily detected in primary rat neurons and human neuronal cells.

A limitation of this study is that we could not correlate RBM5/10 changes with c-FLIP(L/s) and caspase-2(L/s) alterations after CCI+HS. Rodents do not express the c-FLIP(s) variant, precluding its detection in rodent tissues here.[34] However, both c-FLIP(L) and c-FLIP(s) increase after TBI in human brain.[25] Our results show that RBM5 inhibition appears to increase c-FLIP(s) and decrease caspase-2(L) in human neuronal cells. Thus, it is possible that RBM5 inhibition in humans could be a way to further augment c-FLIP(s) after TBI. We also measured caspase-2 in mouse brain homogenates but like human neuronal cells caspase-2(s) was undetectable (data not shown). Future exon microarray studies may reveal other major splicing targets of RBM5 in neurons.

Intron Splicing Factor 1 Is Disturbed after Traumatic Brain Injury

The scope of splicing disturbances after TBI is unknown. A few studies report changes in splicing of a few select proteins after TBI.[35–37] Global splicing derangements could exist if key components of intron splicing are also disturbed. We measured levels of SF1 and SF3A—both important facilitators of intron and exon splicing in cells. Splicing factor 1 protein was markedly decreased in brain after CCI+HS. Levels of SF3A did not decrease below sham. Studies in human cells show that SF1 knockdown induces apoptosis. In contrast, knockdown of the 120-kDa subunit of SF3A (i.e., the subunit measured in our study) induces necrosis.[38] One potential explanation for this difference is that SF3A knockdown also markedly decreases total protein levels in human cells because general loss of pre-mRNA intron splicing decreases translatable mRNAs.[38] In contrast, SF1 depletion only slightly decreases total protein levels—suggesting a more restricted and selective set of intron/exon pre-mRNA gene targets.[38] Regardless the mechanism of cell death, both SF3A and SF1 seem essential for cell viability. Decreased SF1 after CCI+HS may cause intron splicing disturbances, which could affect cellular recovery after injury—whether SF1-dependent splicing disturbances exist after TBI deserves future study. Splicing factor 1 changes have been observed after global brain ischemia in gerbil. In those studies SF1 mRNA acutely peaks 4 hours after ischemia in resistant DG regions but vanished by 4 days in dying hippocampal CA1 subregion.[39] Future studies need to test whether SF1 protein is needed for neuronal viability, and thus if it may represent another important target for splicing therapies in brain.

DISCLOSURE/CONFLICT OF INTEREST

Dr Travis C Jackson and Dr Patrick M Kochanek are inventors on a filed international PCT patent application (#PCT/US2013/040995) titled: 'Small molecule inhibitors of RNA binding motif (RBM) proteins for the treatment of acute cellular injury.'

REFERENCES

1 Schwerk C, Schulze-Osthoff K. Regulation of apoptosis by alternative pre-mRNA splicing. *Mol Cell* 2005; **19**: 1–13.
2 Wang L, Miura M, Bergeron L, Zhu H, Yuan JY. Ich-1 an Ice/Ced-3-related gene, encodes both positive and negative regulators of programmed cell-death. *Cell* 1994; **78**: 739–750.
3 Rappsilber J, Ryder U, Lamond AI, Mann M. Large-scale proteomic analysis of the human spliceosome. *Genome Res* 2002; **12**: 1231–1245.
4 Fushimi K, Ray P, Kar A, Wang L, Sutherland LC, Wu JY. Up-regulation of the proapoptotic caspase 2 splicing isoform by a candidate tumor suppressor, RBM5. *Proc Natl Acad Sci USA* 2008; **105**: 15708–15713.
5 Inoue A, Yamamoto N, Kimura M, Nishio K, Yamane H, Nakajima K. RBM10 regulates alternative splicing. *FEBS Lett* 2014; **588**: 942–947.
6 Wang K, Bacon ML, Rintala-Maki ND, Tang V, Sutherland LC. Rbm10 is a novel modulator of tumour necrosis factor-mediated apoptosis. *Respirology* 2011; **16**: 187–187.
7 Mourtada-Maarabouni M, Sutherland LC, Williams GT. Candidate tumour suppressor LUCA-15 can regulate multiple apoptotic pathways. *Apoptosis* 2002; **7**: 421–432.
8 Han CH, Zhao R, Kroger J, Qu MH, Wani AA, Wang QE. Caspase-2 short isoform interacts with membrane-associated cytoskeleton proteins to inhibit apoptosis. *PLoS ONE* 2013; **8**: e67033.
9 Krueger A, Schmitz I, Baumann S, Krammer PH, Kirchhoff S. Cellular FLICE-inhibitory protein splice variants inhibit different steps of caspase-8 activation at the CD95 death-inducing signaling complex. *J Biol Chem* 2001; **276**: 20633–20640.
10 Bin LH, Li XY, Xu LG, Shu HB. The short splice form of Casper/c-FLIP is a major cellular inhibitor of TRAIL-induced apoptosis. *FEBS Lett* 2002; **510**: 37–40.
11 Micheau O, Thome M, Schneider P, Holler N, Tschopp J, Nicholson DW *et al.* The long form of FLIP is an activator of caspase-8 at the fas death-inducing signaling complex. *J Biol Chem* 2002; **277**: 45162–45171.
12 Bonnal S, Martinez C, Forch P, Bachi A, Wilm M, Valcarcel J. RBM5/Luca-15/H37 regulates Fas alternative splice site pairing after exon definition. *Mol Cell* 2008; **32**: 81–95.
13 Rintala-Maki ND, Sutherland LC. LUCA-15/RBM5, a putative tumour suppressor, enhances multiple receptor-initiated death signals. *Apoptosis* 2004; **9**: 475–484.
14 Wang K, Bacon ML, Tessier JJ, Rintala-Maki ND, Tang V, Sutherland LC. RBM10 modulates apoptosis and influences TNF-α gene expression. *J Cell Death* 2012; **5**: 1–19.
15 Chesnut RM, Marshall LF, Klauber MR, Blunt BA, Baldwin N, Eisenberg HM *et al.* The role of secondary brain injury in determining outcome from severe head injury. *J Trauma* 1993; **34**: 216–222.
16 Hemerka JN, Wu X, Dixon CE, Garman RH, Exo JL, Shellington DK *et al.* Severe brief pressure-controlled hemorrhagic shock after traumatic brain injury exacerbates functional deficits and long-term neuropathological damage in mice. *J Neurotr*2012; **29**: 2192–2208.
17 Jackson TC, Verrier JD, Kochanek PM. Anthraquinone-2-sulfonic acid (AQ2S) is a novel neurotherapeutic agent. *Cell Death Dis* 2013; **4**: e451.
18 Aldridge GM, Podrebarac DM, Greenough WT, Weiler IJ. The use of total protein stains as loading controls: an alternative to high-abundance single-protein controls in semi-quantitative immunoblotting. *J Neurosci Methods* 2008; **172**: 250–254.

19 Li R, Shen Y. An old method facing a new challenge: re-visiting housekeeping proteins as internal reference control for neuroscience research. *Life Sci* 2013; **92**: 747–751.
20 Sutherland LC, Rintala-Maki ND, White RD, Morin CD. RNA binding motif (RBM) proteins: a novel family of apoptosis modulators? *J Cell Biochem* 2005; **94**: 5–24.
21 Salon C, Eymin B, Micheau O, Chaperot L, Plumas J, Brambilla C *et al.* E2F1 induces apoptosis and sensitizes human lung adenocarcinoma cells to death-receptor-mediated apoptosis through specific downregulation of c-FLIP(short). *Cell Death Differ* 2006; **13**: 260–272.
22 Poukkula M, Kaunisto A, Hietakangas V, Denessiouk K, Katajamaki T, Johnson MS *et al.* Rapid turnover of c-FLIP short is determined by its unique C-terminal tail. *J Biol Chem* 2005; **280**: 27345–27355.
23 Spector DL, Lamond AI. Nuclear speckles. *Cold Spring Harb Perspect Biol* 2011; **3**: a000646.
24 Carlsson Y, Schwendimann L, Vontell R, Rousset CI, Wang XY, Lebon S *et al.* Genetic inhibition of caspase-2 reduces hypoxic-ischemic and excitotoxic neonatal brain injury. *Ann Neurol* 2011; **70**: 781–789.
25 Hainsworth AH, Bermpohl D, Webb TE, Darwish R, Fiskum G, Qiu JH *et al.* Expression of cellular FLICE inhibitory proteins (cFLIP) in normal and traumatic murine and human cerebral cortex. *J Cereb Blood Flow Metab* 2005; **25**: 1030–1040.
26 Taoufik E, Valable S, Muller GJ, Roberts ML, Divoux D, Tinel A *et al.* FLIPL protects neurons against In Vivo ischemia and In Vitro glucose deprivation-induced cell death. *J Neurosci* 2007; **27**: 6633–6646.
27 O'Bryan MK, Clark BJ, McLaughlin EA, D'Sylva RJ, O'Donnell L, Wilce JA *et al.* RBM5 is a male germ cell splicing factor and is required for spermatid differentiation and male fertility. *PLoS Genet*2013; **9**: e1003628.
28 Solier S, Logette E, Desoche L, Solary E, Corcos L. Nonsense-mediated mRNA decay among human caspases: the caspase-2S putative protein is encoded by an extremely short-lived mRNA. *Cell Death Differ* 2005; **12**: 687–689.
29 Shariati SA, Lau P, Hassan BA, Muller U, Dotti CG, De Strooper B *et al.* APLP2 regulates neuronal stem cell differentiation during cortical development. *J Cell Sci* 2013; **126**: 1268–1277.
30 Zhang X, Herrmann U, Weyer SW, Both M, Muller UC, Korte M *et al.* Hippocampal network oscillations in APP/APLP2-deficient mice. *PLoS ONE* 2013; **8**: e61198.
31 Weyer SW, Klevanski M, Delekate A, Voikar V, Aydin D, Hick M *et al.* APP and APLP2 are essential at PNS and CNS synapses for transmission, spatial learning and LTP. *EMBO J* 2011; **30**: 2266–2280.
32 Wang YB, Gogol-Doring A, Hu H, Frohler S, Ma YX, Jens M *et al.* Integrative analysis revealed the molecular mechanism underlying RBM10-mediated splicing regulation. *EMBO Mol Med* 2013; **5**: 1431–1442.
33 Cho GW, Shin SM, Kim HK, Ha SA, Kim S, Yoon JH *et al.* HCCR-1, a novel oncogene, encodes a mitochondrial outer membrane protein and suppresses the UVC-induced apoptosis. *BMC Cell Biol* 2007; **8**: 50.
34 Ueffing N, Keil E, Freund C, Kuhne R, Schulze-Osthoff K, Schmitz I. Mutational analyses of c-FLIPR, the only murine short FLIP isoform, reveal requirements for DISC recruitment. *Cell Death Differ* 2008; **15**: 773–782.
35 Yi JH, Pow DV, Hazell AS. Early loss of the glutamate transporter splice-variant GLT-1v in rat cerebral cortex following lateral fluid-percussion injury. *Glia* 2005; **49**: 121–133.
36 Schober ME, Ke X, Xing B, Block BP, Requena DF, McKnight R *et al.* Traumatic brain injury increased IGF-1B mRNA and altered IGF-1 exon 5 and promoter region epigenetic characteristics in the rat pup hippocampus. *J Neurotr*2012; **29**: 2075–2085.
37 Schaible EV, Windschugl J, Bobkiewicz W, Kaburov Y, Dangel L, Kramer T *et al.* 2-Methoxyestradiol confers neuroprotection and inhibits a maladaptive HIF-1alpha response after traumatic brain injury in mice. *J Neurochem* 2014; **129**: 940–954.
38 Tanackovic G, Kramer A. Human splicing factor SF3a, but not SF1, is essential for pre-mRNA splicing in vivo. *Mol Biol Cell* 2005; **16**: 1366–1377.
39 Covini N, Tamburin M, Consalez G, Salvati P, Benatti L. ZFM1/SF1 mRNA in rat and gerbil brain after global ischaemia. *Eur J Neurosci* 1999; **11**: 781–787.
40 von Koch CS, Zheng H, Chen H, Trumbauer M, Thinakaran G, van der Ploeg LH *et al.* Generation of APLP2 KO mice and early postnatal lethality in APLP2/APP double KO mice. *Neurobiol Aging* 1997; **18**: 661–669.

Supplementary Information accompanies the paper on the Journal of Cerebral Blood Flow & Metabolism website (http://www.nature.com/jcbfm)